JMEPEG (2004) 13:575-582
DOI: 10.1361/10599490420584

1059-9495/$19.00

Role of Environmental Variables on the Stress Corrosion Cracking of Sensitized AISI Type 304 Stainless Steel (SS304) in Thiosulfate Solutions

S. Roychowdhury, S.K. Ghosal, and P.K. De

(Submitted June 9, 2003)

The stress corrosion cracking (SCC) behavior of sensitized AISI type 304 stainless steel (SS304) has been studied in dilute thiosulfate solutions as a function of thiosulfate concentrations and applied potentials. The susceptibility to SCC was observed to increase with thiosulfate concentrations and applied potentials. The addition of boric acid produced the reverse effect. A critical potential was found to exist, below which no SCC took place. Potential fluctuations, as recorded in the tests under open circuit conditions, appeared to be correlated with crack initiation and propagation during SCC. Current fluctuations observed in the controlled potential tests also gave indications of crack nucleation; however, at higher applied potentials such fluctuations were absent. The formation and presence of martensite in the specimens seemed to have a minor role in the overall SCC process. The aggressiveness of the thiosulfate concentration was also an important factor in determining the degree of susceptibility to SCC. The results obtained in the slow strain rate tests under open circuit as well as under potential-controlled conditions suggested a film rupture-anodic dissolution type of mechanism operative during SCC of sensitized SS304 in thiosulfate solutions.

Keywords AISI type 304 stainless steel (SS304), martensite formation, potential control, sensitization, stress corrosion cracking, thiosulfate solution

1. Introduction

The stress corrosion cracking (SCC) behavior of sensitized AISI type 304 stainless steel (SS304) in dilute thiosulfate solutions has been studied by various workers in the past. The interest in such a system might arise from the fact that very dilute and neutral solutions of thiosulfate have been observed to induce cracking.[1-4] Thiosulfate may be found in various environments and can be formed in certain environments by sulfate-reducing bacteria. Newman et al.[3] reported that grain boundary cracking through a zone containing strain-generated martensite most probably constituted the majority of crack propagation in the stage II regimen, and this was possibly, but not necessarily, associated with hydrogen. Isaacs[5] tried to correlate the observed potential fluctuations with the initiation of SCC. He noticed a marked decrease in specimen potential due to the onset of cracking. There was a drop in potential if the cracks remained active. However, repassivation of the cracks once again raised the potential. Wells et al.[6] developed the idea of microstructural barriers to the propagation of short stress corrosion cracks. They stated that such barriers became less important as the chemistry of the environment became more aggressive. They also concluded that strain-induced martensite formation resulted in a decrease, with increasing strain, in both microcrack nucleation frequency and penetration.

S. Roychowdhury, S.K. Ghosal, and **P.K. De,** Materials Science Division Bhabha Atomic Research Centre, Trombay, Mumbai 400 085, India. Contact e-mail: skghosal@apsara.barc.ernet.in.

The electrochemical potential and current measurements during SCC and other localized corrosion processes have been useful in defining and understanding the mechanism of SCC[5,7] and have been used to elucidate the cracking behavior in many metal-environment systems. In the present investigation, these methods were used to further understand the extent of electrochemical parameters (potential and current), metallurgical factors (sensitized microstructure and martensite formation), and mechanical factors (effect of stress on crack growth) on stress corrosion failure of sensitized SS304 in thio sulfate solutions. As an extension of this work, the SCC behavior in the presence of boric acid (H_3BO_3) also was investigated.

2. Experimental

SS304 rods of commercial purity were used in this investigation. The chemical composition of the steel was: carbon (C) (0.06 wt.%), chromium (Cr) (18.28 wt.%), nickel (Ni) (8.44 wt.%), manganese (Mn) (1.65 wt.%), silicon (Si) (0.47 wt.%), sulfur (S) (0.024 wt.%), phosphorus (P) (0.036 wt.%), and iron (Fe) (bal). Standard round and smooth tensile specimens, as shown in Fig. 1, were machined from these rods. The machined specimens then were sealed in silica tubes, annealed at 1050 °C for 15 min, and water quenched. The annealed specimens, while in silica tubes, were further sensitized at 650 °C for 2 h and again water quenched. The grain size of the annealed material was found to be about 75 μm, while the 0.2% proof stress and ultimate tensile strength (UTS) were measured to be 206 and 768 MPa, respectively.

Electrochemical potentiokinetic reactivation (EPR) tests, conducted in a solution containing 0.5 *M* H_2SO_4 + 0.01 *M* KSCN to find the degree of sensitization of the SS304, showed complete attack around all grain boundaries with the degree of sensitization equal to 17%. Figure 2 shows the evolution of microstructure after the EPR test.

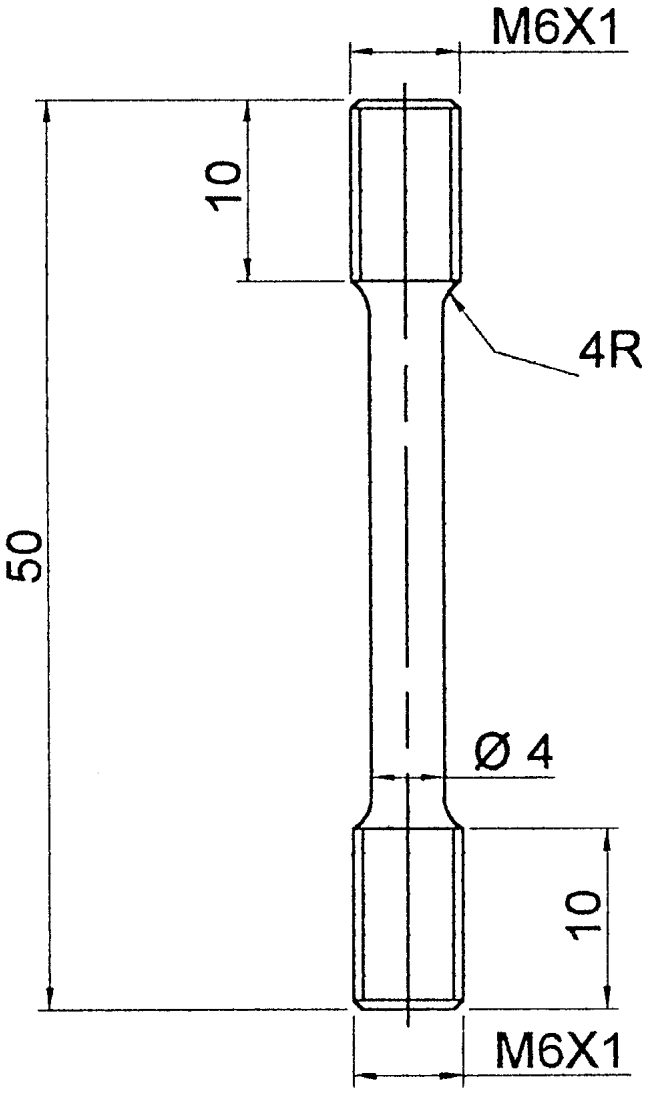

Fig. 1 Geometry of SCC test specimens. All dimensions are in millimeters.

Slow strain rate tests (SSRTs) were carried out at a fixed strain rate of 10^{-6}s in thiosulfate solutions (1-1000 ppm $Na_2S_2O_3$) at room temperature with or without boric acid. Guaranteed reagent (GR) grade $Na_2S_2O_3$ and H_3BO_3 were used for the preparation of solutions. The pH of the thiosulfate solutions was maintained in the range of 6-7. With the addition of boric acid, the resultant pH decrease to 3-4.

All the SCC tests were carried out in a glass vessel that was open to the air. A potentiostat was used for the application of potentials to the specimens, and a data logger was used to record potential and current. Potentials were measured and recorded with respect to a calomel electrode. A platinum sheet served as the counter electrode. Before each test, the specimens were abraded in the longitudinal direction on 600 grit SiC paper and degreased in acetone. After the tests, the specimens were examined in optical and scanning electron microscopes.

For the electrochemical polarization tests, the solutions were purged with argon gas before and during the tests. For the purpose of comparison, some of the tests were carried out without argon purging. A potentiostat-galvanostat was used for these tests, employing a scan rate of 20 mV/min. All test specimens were polished on different grades of emery paper, and ultimately on a polishing wheel using 0.5 μm diamond paste, to obtain mirror-finish surfaces.

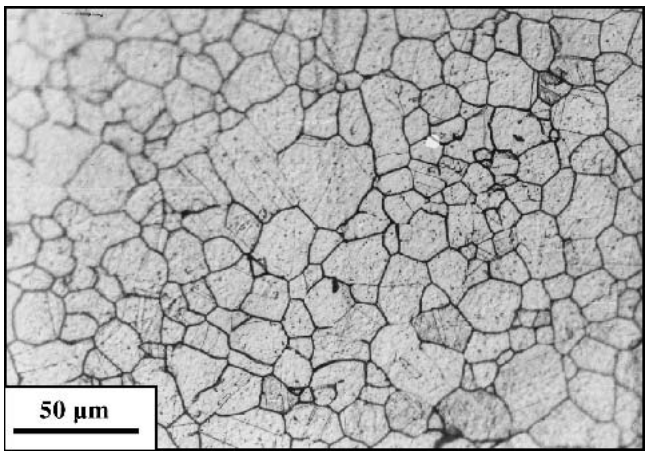

Fig. 2 Microstructure of SS304 after the EPR test

3. Results

3.1 Polarization Tests

The polarization diagrams obtained in 1, 10, and 100 ppm thiosulfate solutions are shown in Fig. 3(a) and (b). With the increase in thiosulfate concentrations, there was not much change in the shape of the polarization diagrams. Passive current densities on the order of 10^{-7} A/cm^2 were recorded in all these solutions. In 10 and 100 ppm solutions, passive current densities were a little higher than that in 1 ppm solution. Deaeration of the solutions resulted in a shifting of the open circuit potentials (OCPs) to more active values. In solutions open to air, the OCP values were in the range of 0 to −100 mV. Deaeration shifted these potentials to around −250 mV. The passive region was stable until an applied potential of +1000 mV was reached. Optical microscopic examination after the polarization runs did not reveal any specific corrosion attack on the specimens.

In the presence of 0.36 *M* boric acid, the nature of the polarization diagrams was similar in the different thiosulfate solutions. These diagrams are shown in Fig. 4. The OCPs shifted slightly toward positive values in solutions containing 1-10 ppm thiosulfate compared with those formed in the absence of boric acid and were in the range of −100 to −200 mV. The passive current densities were again of the order of 10^{-7} A/cm^2.

3.2 SSRT Under Open Circuit Conditions

Figure 5 shows the variations in maximum loads at the failure of sensitized SS304 in thiosulfate solutions. In solutions containing 1 ppm thiosulfate, there was ductile failure, with no apparent SCC. With an increase in thiosulfate concentrations,

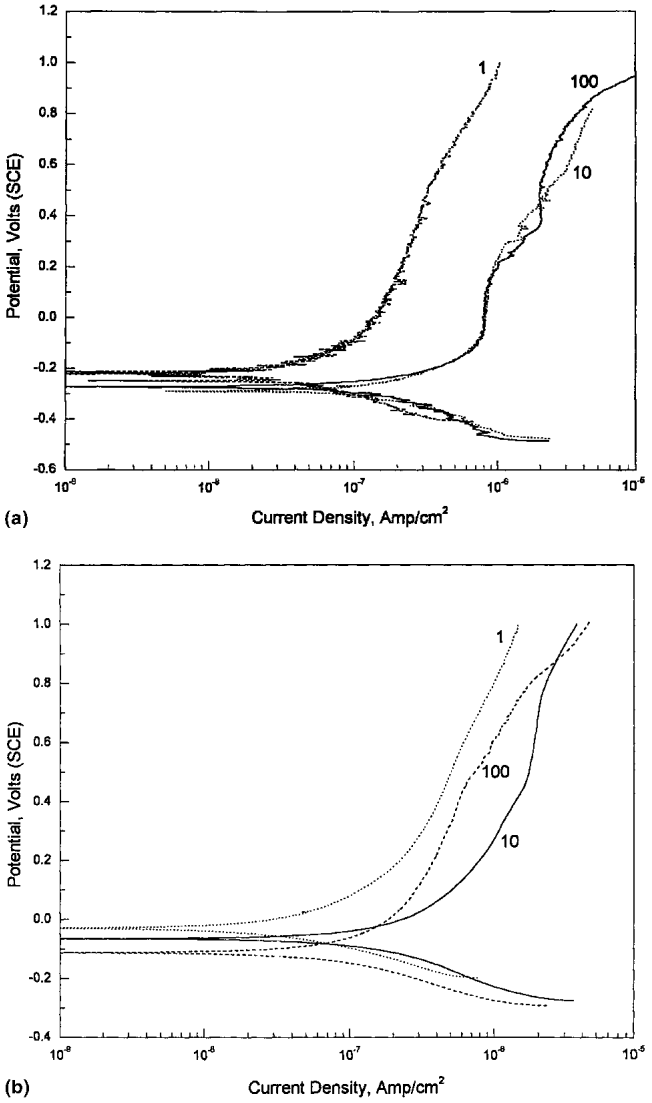

Fig. 3 Potentiodynamic polarization diagrams for sensitized SS304 in 1, 10, and 100 ppm thiosulfate solutions. **(a)** deaerated; **(b)** open to air

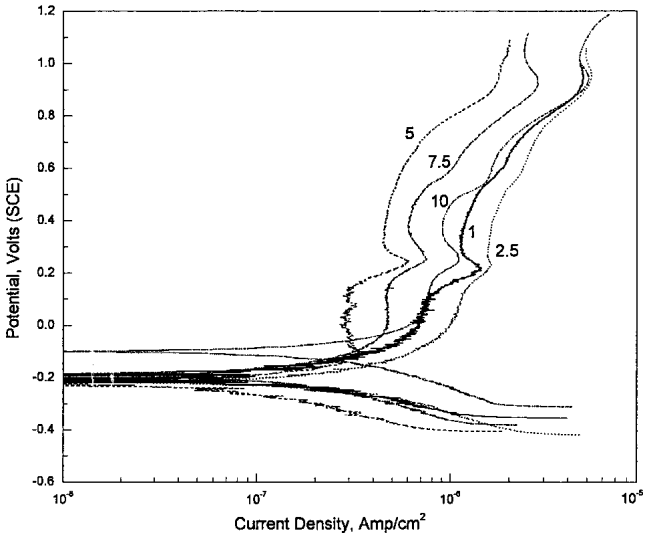

Fig. 4 Polarization diagrams for sensitized SS304 in different thiosulfate solutions, each containing 0.36 *M* boric acid. The numbers by the side of the curves indicate thiosulfate concentrations in ppm.

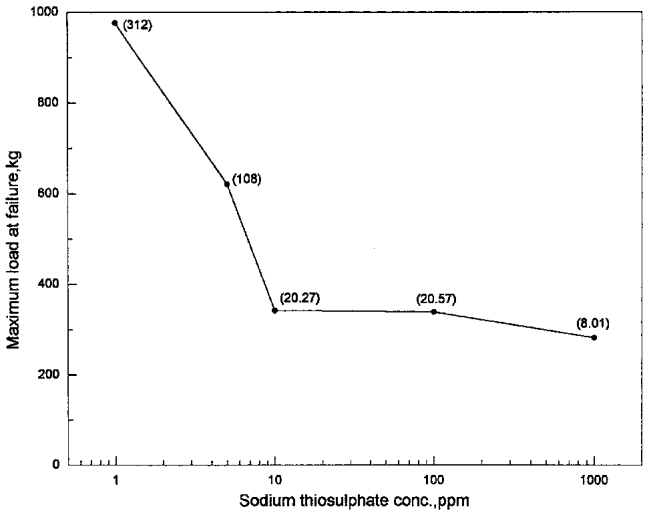

Fig. 5 Variations in maximum load at failure with thiosulfate concentrations. The numbers in brackets indicate the time to failure in hours.

the maximum load at failure, and also, correspondingly, the time to failure, gradually decreased due to SCC. From 10 ppm onward, the specimens failed within a few hours. Complete intergranular cracking was noticed on the fracture surfaces of all these specimens, as is shown in Fig. 6.

There was no secondary cracking in any specimen except for the one in the 1000 ppm solution in which two or three fine secondary cracks near the main crack were noticed. In the other solutions, only one crack initiated and propagated across the gauge length. Though there was some discoloration of the fracture surfaces, the gauge lengths remained bright and shiny in all the solutions.

The potentials of the specimens were monitored during tests conducted under open circuit conditions in solutions containing 1-100 ppm thiosulfate, and variations in potentials with time are shown in Fig. 7.

In the 1 ppm solution, as shown in Fig. 7(a) where ductile failure was noticed, after some initial fluctuations, the potential of the specimens became nearly stable within the range 0 to −50 mV. In 5 ppm solution (Fig. 7b), after an initial rise the potential became stable at around −250 mV. Some potential fluctuations of short height were recorded in this solution. In 10 and 100 ppm solutions (Fig. 7c and d, respectively), a few well-differentiated potential peaks were observed. However, these peaks decayed to around −200 to −250 mV with time and remained the same until the final fracture.

3.3 SSRT Under Potential Control

Figure 8 shows the effects of applied potentials on the SCC behavior of sensitized SS304 in 10 ppm thiosulfate solutions. At an applied potential of −300 mV, there was ductile failure.

However, with the application of more positive potentials, the susceptibility to cracking increased, and a gradual decrease in maximum load at failure was noticed. In the potential range of −100 to +500 mV, specimens were observed to fail within about 14 h.

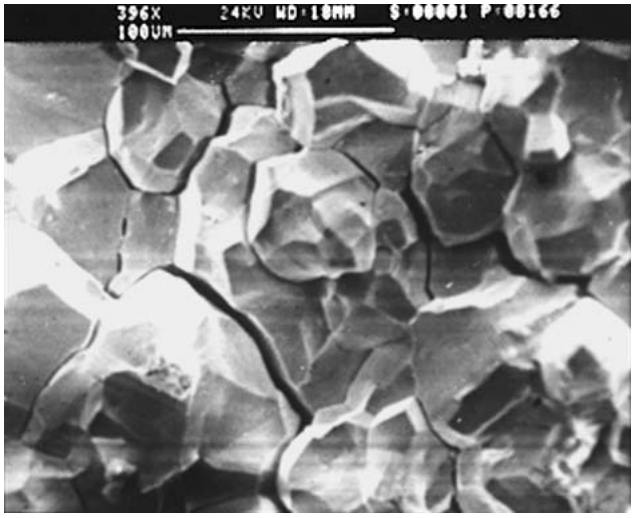

Fig. 6 Scanning electron microscope (SEM) micrograph showing intergranular SCC of sensitized SS304 in thiosulfate solutions

The variations in currents during some of these tests were recorded and have been presented in Fig. 9. At −300 mV, there was initially a sharp increase in current; however, later on during the test the current decayed to an average value of −22 μA. Throughout this test, the current associated with the applied potential was cathodic in nature. At higher applied potentials, starting from −200 mV, the current was stable and positive. It continued to increase until final fracture. Anodic currents on the order of μA were recorded in all of these experiments. Similar trends in the current versus time plots have been recorded by other workers, including Kawashima et al.,[8] who examined different metal-environment systems.

3.4 Effect of Boric Acid

The effects of boric acid additions on the susceptibility to cracking are shown in Fig. 10, where 0.36 *M* boric acid was added to different thiosulfate solutions. For the purpose of comparison, the data from Fig. 5 have been replotted in Fig. 10. In the 1 and 2.5 ppm solutions, ductile failure was noticed in the presence of boric acid. However, the addition of boric acid could not stop SCC in solutions containing higher amounts of

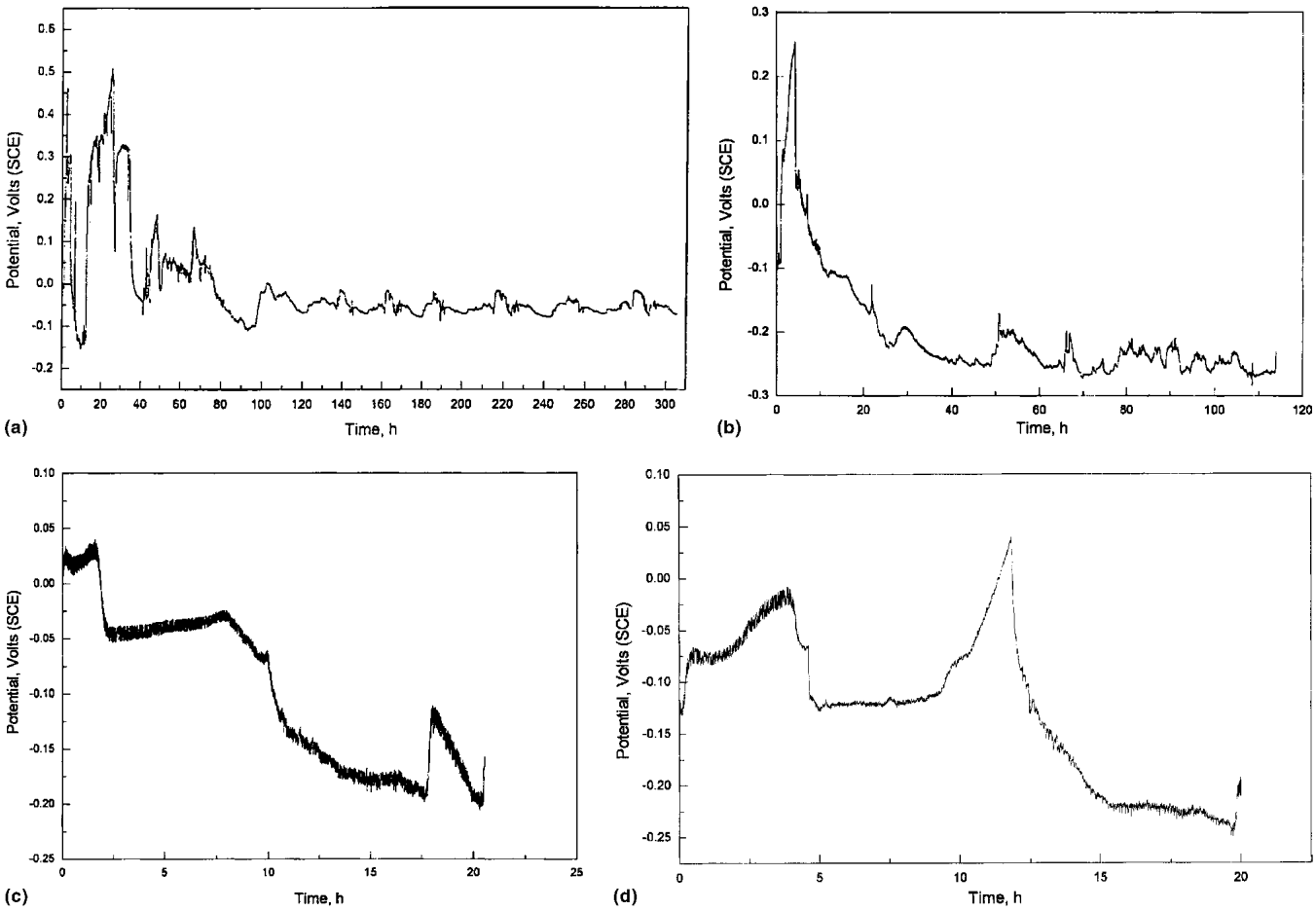

Fig. 7 Variations in the potentials of specimens with time in SCC tests conducted under open circuit conditions in different thiosulfate solutions. **(a)** 1 ppm; **(b)** 5 ppm; **(c)** 10 ppm; and **(d)** 100 ppm

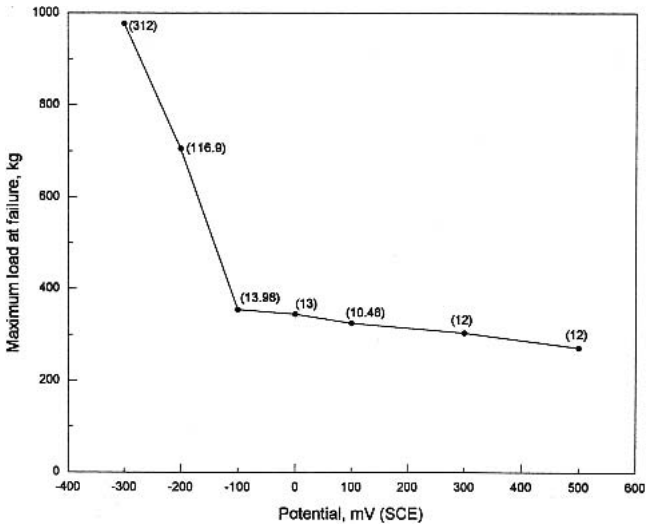

Fig. 8 The effect of applied potentials on the maximum loads at the failure of sensitized SS304 specimens in the 10 ppm thiosulfate solution. The numbers in brackets indicate the time to failure in hours.

thiosulfate. Thus, in 5-100 ppm thiosulfate solutions SCC was observed. The times to failure gradually decreased with the increase in thiosulfate concentrations. Boric acid additions, though, resulted in a marked reduction in the susceptibility to cracking. Thus, for 5 and 10 ppm solutions, and in the presence of boric acid, the times to failure were noticed to be 182 and 110 h, respectively, compared with 108 and 20 h, respectively, in the absence of boric acid. Boric acid was observed to have the ability to drastically reduce the susceptibility to SCC. With further increase in thiosulfate concentrations to 100 ppm, there was no such reduction in SCC susceptibility. The times to failure were observed to be around 13 and 20 h, respectively, in the presence and absence of boric acid.

4. Discussion

Under the open circuit conditions, it was observed that the susceptibility of sensitized SS304 toward SCC increased with the thiosulfate concentrations. An examination of the specimens after the EPR tests showed that the grain boundaries were affected or attacked during these tests. Thus, from the standpoint of the presence of an active path, the grain boundaries in the material seemed to be equally susceptible to SCC. The polarization diagrams in the 1-100 ppm solutions were similar in nature, giving rise to passive current densities of the order of 10^{-7} A/cm^2. As a consequence, the degree of susceptibility to cracking in the above solutions could not be predicted from these diagrams.

4.1 SCC Under OCPs

In 1 ppm solution in which ductile failure was observed, after some initial increase/fluctuations, the potential leveled off and almost became stable around the initial corrosion potential. In 5-100 ppm solutions, the potentials were observed to have a tendency to be stable around −200 to −250 mV, at which point the final failures were observed to have taken place. However, in these solutions, particularly in the solutions containing higher amounts of thiosulfate, a number of potential peaks were noticed. The frequency of fluctuations decreased with the increase in thiosulfate concentrations. Such potential fluctuations could be correlated with crack initiation and propagation, as has been observed by Isaacs.[5] He noticed a marked and continuous decrease in potential if cracking remained active and an increase in potential when cracks repassivated. In the present investigation in all solutions containing 5-100 ppm thiosulfate, only one crack was observed to initiate and propagate. There was no secondary crack formation, although potential fluctuations were observed in each of these tests. It seems that even if one crack initiated and propagated, depending on the actual electrochemical conditions inside the crack, it was possible to have potential fluctuations as it grew, ultimately leading to failure. Given the presence of stress, whether a single crack initiates and propagates will depend on the metallurgical and chemical conditions inside the crack. In the present case, due to the sensitized nature of the material, the metallurgical condition is met, and, due to the presence of thiosulfate, the chemical conditions are also met. Thus, a single crack initiated and propagated through the material. The presence of other initiation sites was not required. It should also be noted that such potential fluctuations may not be observable for every metal-environment system. Mom et al.[9] did not observe any potential fluctuations while conducting tests with SS304 in 35.5% $MgCl_2$ solutions. However, the presence of potential fluctuations in thiosulfate solutions has also been reported by Wells et al.[6] for sensitized SS304. They observed a sustained decrease in the corrosion potential with the nucleation and growth of a visible large crack in heavily sensitized specimens.

4.2 SCC Under Controlled Potentials

The observation of current variations during SCC may be another aspect of monitoring crack growth. In the case of ductile failure at −300 mV, a cathodic current was involved, thus making the sensitized material resistant to SCC. However, positive currents were involved right from the beginning of the other experiments in which SCC took place. At −200 mV, many short fine cracks, as shown in Fig. 11, were noticed along the gauge length. The current fluctuations recorded in this experiment could be related to the nucleation of fine cracks or due to the movement of a crack across a single grain boundary facet, as observed by Wells et al.[6] Such current fluctuations were almost absent in experiments conducted at higher applied potentials. It could be that currents produced by a few deep cracks overshadow the effects of other fine cracks.

4.3 General Discussion

The addition of boric acid improved the resistance of the sensitized SS304 to SCC. However, when a certain concentration of thiosulfate was exceeded, the boric acid addition became ineffective. It was noticed that in the presence of boric acid for the 5 and 100 ppm solutions, there was only one crack, which initiated and then propagated. In the 7.5 and 10 ppm solutions, many short and wide-open cracks formed. In the absence of boric acid, there were mostly single cracks with no

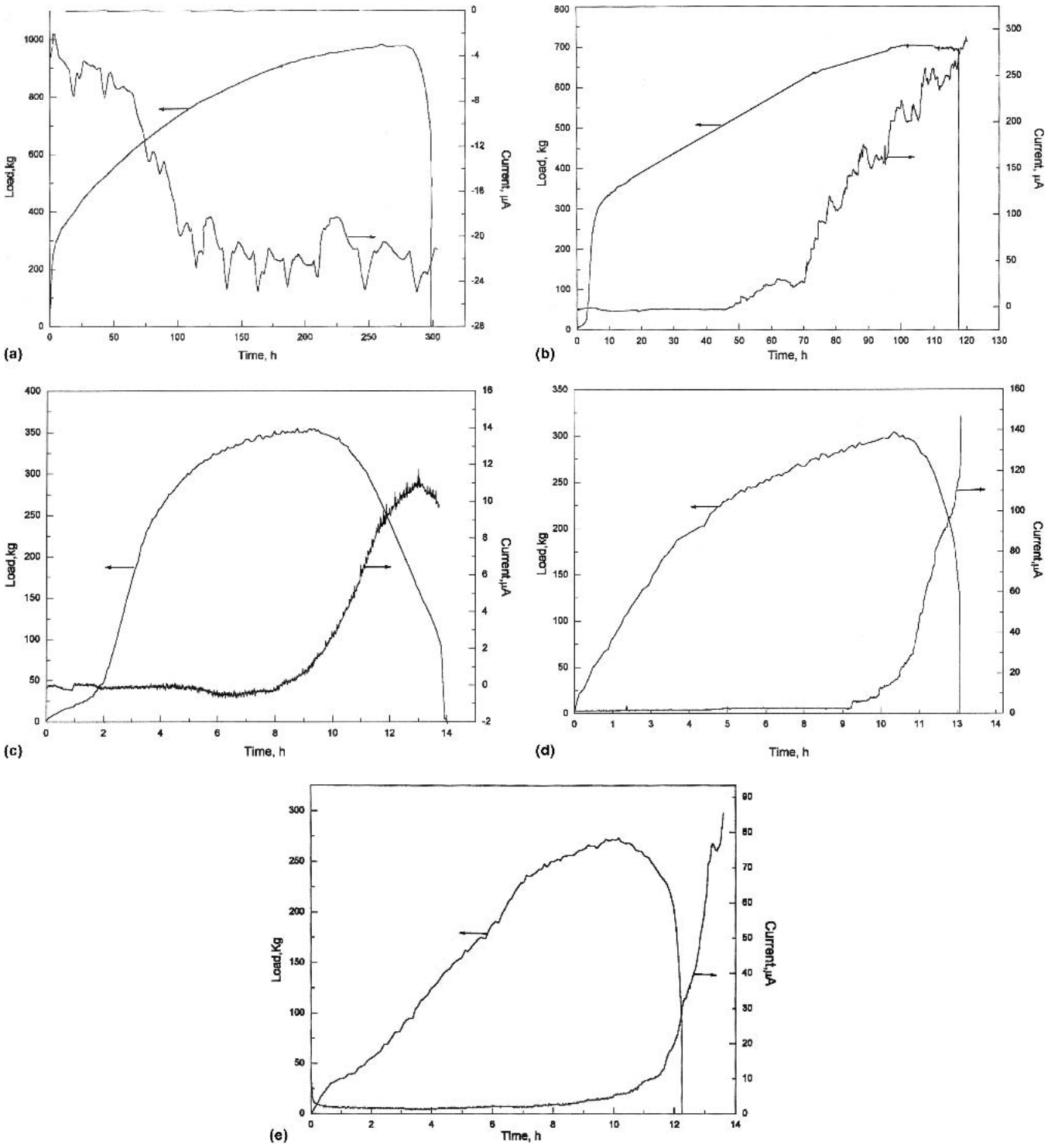

Fig. 9 Variations in current recorded under different applied potentials in 10 ppm thiosulfate solution. **(a)** −300 mV; **(b)** −200 mV; **(c)** −100 mV; **(d)** +300 mV; and **(e)** +500 mV

secondary cracking. However, under the application of potentials in the 10 ppm solution, and at −200 to +500 mV, a number of cracks nucleated in the specimens.

Crack nucleation and propagation are two different aspects of SCC. In the absence of boric acid, a single crack can sustain proper electrochemical conditions and propagate to failure. On the other hand, certain environments may lead to multiple crack nucleation as was observed at −200 mV, and also in 7.5 and 10 ppm solutions in the presence of boric acid. However, with reduced crack propagation rates, the specimens took a

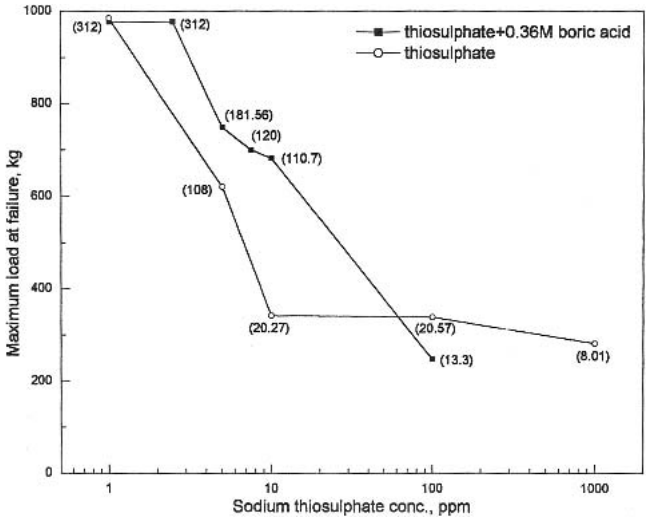

Fig. 10 The effect of boric acid additions on the maximum loads at the failure of sensitized SS304 in different thiosulfate solutions. The numbers in brackets indicate the time to failure in hours.

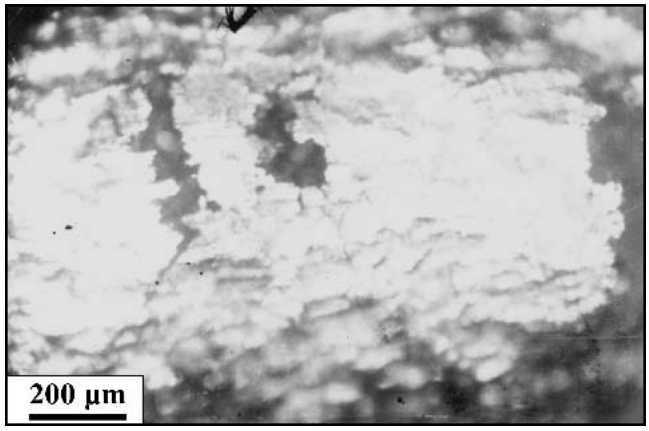

Fig. 11 The formation of short fine cracks in a sensitized specimen held at −200 mV in a 10 ppm thiosulfate solution

longer time to fail under these conditions. At +500 mV, the aggressive environmental condition led to the nucleating of numerous cracks; however, the crack propagation rate was quite high, reducing the time to failure. Thus, SCC of the sensitized steel was observed to be dependent on thiosulfate concentrations and was also completely electrochemically controlled.[10]

Film rupture and anodic dissolution seemed to be the most appropriate mechanisms of failure in thiosulfate solutions. A balance between the film rupture and film formation could be controlled by the aggressive ion concentration as well as by the application of potentials. Depending on the aggressive nature of the environment and/or the electrochemical conditions, the rates of crack nucleation and crack propagation will vary. Eventually, however, it is the crack propagation rate that decides the degree of susceptibility to cracking.

It is well known that the mechanical[11] and corrosion[12,13] properties of austenitic stainless steels are strongly affected by

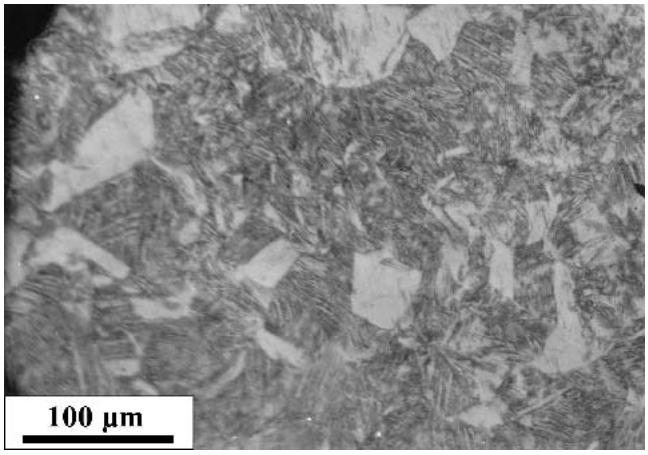

Fig. 12 Optical micrograph showing the presence of martensite in a specimen after the SCC test

the deformation-induced martensite transformation. At a true strain value of 0.15, Narutani[11] reported that transformation to α-martensite became active in SS301. He also reported martensite formation along certain crystallographic planes, extending from the one grain boundary to the other across the grain interior. These features were initially thought to be slip planes. Newman et al.[3] reported extensive martensite both at grain boundaries and within the grains in SS304, and, while developing a mechanism of crack growth in thiosulfate solutions, they have involved martensite formation at a distance ahead of the crack tip in the crack propagation process. Wells et al.[6] also concluded that the frequency of microcrack formation was related to strain-induced martensite formation. In the present investigation, the fracture surfaces of all the specimens were observed to be attracted toward a magnet. Moreover, parts of the gauge lengths on both sides of the main crack were seen to be magnetic, while the threaded heads and the shoulders of the specimens were not at all attracted toward the magnet. These observations confirmed to a certain extent the presence of deformation-induced martensite in all tested specimens.

The gauge length portions of some of the tested specimens were polished and etched in a solution containing $CuCl_2$, HCl, ethanol, and water. Optical microscopic examination of these specimens showed the presence of martensite in the microstructures, as shown in Fig. 12. However, the experimental results obtained point to the fact that it is the electrochemical conditions before the onset of cracking as well as during crack growth, and inside the cracks, that are responsible for the overall crack growth of the alloy and its susceptibility to cracking. It is the electrochemical dissolution that is responsible for the initiation of a crack as well as for the formation and maintenance of a sharp crack tip of high stress concentration. After a certain level of stress develops, the applied load opens the crack, which then propagates. This process is repeated until final failure. Depending on the aggressiveness of the environment or the electrochemical conditions, it is possible to have a single crack cause failure. It is also possible to have multiple cracks nucleate with long times to failure under similar applied loading conditions, as has been observed in the present investigation. Thus, at −200 mV applied potential, although exten-

sive martensite formation was expected in the specimen, it took a long time (about 117 h) for the specimen to fail, showing the negligible effect of martensite on crack propagation, even in the presence of many nucleated cracks along the specimen gauge length.

Olsen and Cohen[14] reported that grain boundaries are the preferred sites for martensite nucleation. In the presence of grain boundary martensite, the initiation of cracks is affected by the subsequent deformation in the martensite and by the generation of slip steps. Both mechanisms occur less frequently in martensite than in austenite, thus leading to increased times to failure or reduced susceptibility. However, in the 10 and 100 ppm solutions the sensitized SS304 failed immediately after reaching the yield strength, showing the effect of the aggressiveness of these solutions. In fact, this should not have happened if martensite was involved in the crack initiation and propagation stages, as has been observed by various researchers.[15-19] Due to the positive volume change due to the γ-α (martensite) transformation at the crack tip plastic zone, a compressive stress develops at the crack tip, which reduces the effective stress intensity and retards the fatigue crack growth rate at low applied stresses, or in the low ΔK range.

It has been noted by various workers[3] that the SCC velocity is often much higher than that predicted from the electrochemical dissolution data. It seems that in such cases the contribution of stress in opening up a crack is not accounted for. The nucleation of a defect/crack is not sufficient for crack propagation. As noted above, a critical level of stress is required at the tip of the crack, so that the crack will continue to propagate. The dissolution current peak resulting from the creation of fresh surfaces may not be sufficient to account for the crack growth under stress. Thus, an anomaly is expected between the observed crack velocity and that predicted by the electrochemical dissolution.

5. Conclusions

- SS304 sensitized at 650 °C for 2 h was observed to be susceptible to SCC in the thiosulfate solutions.
- An increase in the thiosulfate concentrations increased the susceptibility to cracking.
- Electrochemical conditions influenced the degree of susceptibility of the sensitized steel to SCC. Application of potential below a critical value resulted in ductile failure.
- The observed potential peaks in the tests under OCP conditions seemed to correlate with crack nucleation and propagation.
- The monitoring of current during crack growth under constant applied potentials showed a monotonic increase in current until failure.
- The whole process of crack initiation and crack propagation could well be described by the presence of a sensitized structure (active path) and the prevailing aggressiveness of the solution or electrochemical conditions. Film rupture and anodic dissolution could contribute to cracking.

Acknowledgment

The authors express their gratitude to Dr. S. Banerjee, Director, Materials Group, Bhabha Atomic Research Centre, for his encouragement and useful suggestions during the course of this investigation.

References

1. G. Cragnolino and D.D. Macdonald, Intergranular Stress Corrosion Cracking of Austenitic Stainless Steels at Temperatures Below 100 °C—A Review, *Corrosion,* Vol 38 (No. 8), 1982, p 406-424
2. H.S. Isaacs, BWR Water Chemistry Projects Review Meeting, *EPRI,* 13-14 May 1980 (Palo Alto, CA)
3. R.C. Newman, K. Sieradzki, and H.S. Isaacs, Stress-Corrosion Cracking of Sensitized Type 304 Stainless Steel in Thiosulphate Solutions, *Metall. Trans.,* Vol 13A, 1982, p 2015-2026
4. R.C. Newman, R. Roberge, and R. Bandy, Environmental Variables in the Low Temperature Stress Corrosion Cracking of Inconel 600, *Corrosion,* Vol 39 (No. 10), 1983, p 386-390
5. H.S. Isaacs, Initiation of Stress Corrosion Cracking of Sensitized Type 304 Stainless Steel in Dilute Thiosulphate Solution, *J. Electrochem. Soc.,* Vol 135 (No. 9), 1988, p 2180-2183
6. D.B. Wells, J. Stewart, R. Davidson, P.M. Scott, and D.E. Williams, The Mechanism of Intergranular Stress Corrosion Cracking of Sensitized Austenitic Stainless Steel in Dilute Thiosulphate Solution, *Corros. Sci.,* Vol 33 (No. 1), 1992, p 39-71
7. R.C. Newman, K. Sieradzki, and J. Woodward, *Corrosion Chemistry, Pits, Crevices and Cracks,* A. Turnbull, Ed., HMSO, 1987, p 203
8. A. Kawashima, A.K. Agrawal, and R.W. Staehle, *Stress Corrosion Cracking: The Slow Strain Rate Technique,* STP 665, G.M. Ugiansky and J.H. Payer, Ed., ASTM, 1979, p 266-278
9. A.J.A. Mom, R.T. Dencher, C.J. v.d. Wekken, and W.A. Schultze, *ibid.,* p 305-319
10. H.S. Isaacs, B. Vyas, and M.W. Kendig, The Stress Corrosion Cracking of Sensitized Stainless Steel in Thiosulfate Solutions, *Corrosion,* Vol 38 (No. 3), 1982, p 130-136
11. T. Narutani, Effect of Deformation-Induced Martensitic Transformation on the Plastic Behavior of Metastable Austenitic Stainless Steel, *Mater. Trans., JIM,* Vol 30 (No. 1), 1989, p 33-45
12. K. Elayaperumal, P.K. De, and J. Balachandra, Passivity of Type 304 Stainless Steel: Effect of Plastic Deformation, *Corrosion,* Vol 28 (No. 7), 1972, p 269-273
13. C. Hahin, R.M. Stoss, B.H. Nelson, and P.J. Reucroft, Effect of Cold Work on the Corrosion Resistance of Nonsensitised Austenitic Stainless Steels in Nitric Acid, *Corrosion,* Vol 32 (No. 6), 1976, p 229-238
14. G.B. Olsen and M.A. Cohen, A General Mechanism of Martensitic Nucleation: Part I General Concepts and the FCC-HCP Transformation, *Metall. Trans.,* Vol 7A, 1976, p 1897-1904
15. G.R. Chanani, S.D. Antolovich, and W.W. Gerberich, Fatigue Crack Propagation in Trip Steel, *Metall. Trans.,* Vol 3A, 1972, p 2661-2672
16. C. Bathias and R.M. Pelloux, Fatigue Crack Propagation in Martensitic and Austenitic Steels, *Metall. Trans.,* Vol 4A, 1973, p 1265-1273
17. A.G. Pineau and R.M. Pelloux, Influence of Strain-Induced Martensite Transformations on Fatigue Crack Growth Rates in Stainless Steels, *Metall. Trans.,* Vol 5A, 1974, p 1103-1112
18. G. Franke and C.J. Altstetter, Low Cycle Fatigue Behavior of Mn/N Stainless Steels, *Metall. Trans.,* Vol 7A, 1976, p 1719-1727
19. Z. Khan and M. Ahmed, Stress-Induced Martensitic Transformation in Metastable Austenitic Stainless Steels: Effect of Fatigue Crack Growth Rate, *J. Mater. Eng. Perf.,* Vol 5 (No. 2), 1996, p 201-208